Supporting Information

Supporting Information Corrected July 05, 2013
Shinohara *et al.* 10.1073/pnas.0807461105

SI Materials and Methods

Lentivirus Injection Guided by *In Vivo* Electrophysiology. Nine-week-old mice were anesthetized with ketamine (200 mg/kg) and xylazine (2.5 mg/kg) and the skull of the animal was fixed in a stereotaxic apparatus. The body temperature of the mouse was kept at 37 °C by placing a small heat pad. A small craniotomy (diameter, 1.5 mm) was made at a stereotaxic coordinate of anteroposterior −2.0 mm and lateral 2.6 mm from the bregma. Electrode was made from a thick wall boro-silicate glass pipette (1B150F-4; World Precision Instruments), and the tip was broken so that the diameter of the electrodes should be 10 to 20 μm. Lentivirus suspended in Hepes-Hanks solution was filled from the tip, and then saline solution was filled from the shank. The electrode was attached to an electronically driven fine manipulator (EMM-3; Narishige), and progressed slowly into the brain with an insertion angle of −80°. The fine manipulator controller unit provided a digital reading that indicated the depth of electrode progression. Extracellular neural activity was monitored through the virus containing electrode using with a computer programmable DC bridge amplifier (Multiclamp 700B; Axon Instruments), and stored on a hard drive using custom-build software written with LabVIEW (National Instruments; 20 kHz sampling rate, 16-bit resolution). After frequent CA3 multiunit activity was found with characteristic local field gamma (30–80 Hz) oscillation patterns (Fig. S7), lentivirus was injected with gradually increasing air pressure as high as 30 psi (Picospritzer; General Valve). The scalp was sutured and gentamycin was locally applied at the surgical site. Experimental protocols were approved by the RIKEN Institutional Animal Care and Use Committee.

Analysis of CA1 Spine Morphology of Virus-Injected Mice. Mice were deeply anesthetized by pentobarbital (60 mk/kg i.p.) and transcardially perfused with a fixative containing 4.0% paraformaldehyde (PFA), 0.05% glutaraldehyde, and 1.0% picric acid in 0.1 M phosphate buffer (PB; pH 7.4) for 12 min. Brain sections were first incubated in 20% normal goat serum (NGS) diluted in Tris-buffered saline (TBS) solution for 30 min and then incubated in an anti-GFP antibody (mFX73) (1) diluted in TBS solution containing 3% NGS for 24 h. Subsequently, the sections were washed in TBS solution and incubated overnight in TBS solution with 1.0% NGS and biotinylated goat anti-mouse antibody (diluted 1:100; Vector Laboratories). After washes in TBS solution, the sections were incubated in ABC complex (Vector Laboratories) made up in TBS solution and then washed in Tris buffer (pH 7.4). Peroxidase was visualized with diaminobenzidine (0.05% in Tris buffer) using 0.0001% H_2O_2 as a substrate for 10 min. The sections were treated with 1% OsO_4 in PB for 40 min, washed in PB and distilled water, and then contrasted in uranyl acetate for 40 min. They were dehydrated in a series of ethanol and propylene oxide and flat embedded in epoxy resin (Durcupan ACM; Sigma-Aldrich). After polymerization, corresponding small parts (0.5 × 0.5 mm) of the middle SR of the CA1 area in the left and right dorsal hippocampus (bregma, −1.94 mm) were trimmed. Ultra-thin sections were cut at 70 nm thickness using an ultra-microtome (Reichert Ultracut UCT; Leica) and observed with a Tecnai 10 electron microscope (FEI) or EM208S electron microscope (Philips).

PSD areas were calculated by total PSD length appeared in the serial images multiplied by 70 nm thickness. Synaptic volumes were calculated according to the formula of ellipsoidal bodies ($V = 4\pi/3abc$), where a is the maximum spine head radius parallel to PSD; b is the maximum spine head radius orthogonal to PSD; and c is numbers of sections containing the spine head multiplied by 70 nm thickness, divided by 2. Mushroom-type synapses were defined as spines that have perforated PSDs.

Three-dimensional reconstruction of spine head was done using Reconstruct software (John C. Fiala, Boston, MA) from serial section digital images.

VHC Transection. To examine synapses made by ipsilateral Schaffer collateral fibers selectively, VHC was transected as described previously (2) with some minor modifications 5 days before preparation of PSD fraction or fixation for replica labeling. Nine-week-old C57/BL6 mice were deeply anesthetized by pentobarbital (60 mg/kg i.p.) and held in a stereotaxic apparatus. A small piece of razor blade (2.2 mm wide) was glued onto a rod that was clamped on a micromanipulator. From an opening (3 mm wide and 4 mm long, including the bregma) made in the skull, the blade was inserted 4.5 mm vertically at the midline of the brain to transect the VHC. To avoid damaging the sagittal sinus, the blade was initially shifted 0.25 mm to the left or right and inserted 0.20 mm into the cerebral cortex and was then returned to the midline position as the blade was lowered. After slowly removing the blade, a piece of skull was returned to the hole, and the scalp was closed with sutures. For all animals used in this study, complete transection of VHC (bregma, −0.22 to −0.82 mm) was confirmed in 350-μm-thick horizontal serial slices. After operation, gentamycin was locally administered, and penicillin and streptomycin were supplied with drinking water. In accordance with the animal experiment committee of the National Institute for Physiological Sciences (Okazaki, Japan), all efforts were made to minimize animal suffering and reduce the number of animals used.

Immunoblotting. CA1 SR was dissected from 400-μm-thick coronal slices prepared from animals 5 days after the VHC transection. Purification of PSD fraction was performed as described previously (2, 3) using 22, 26, and 18 mice. Briefly, pooled tissues were homogenized in Hepes-buffered 0.32 M sucrose, and nuclear fraction was removed by centrifugation. Crude membrane fraction was collected by 10,000 × g centrifugation, and the pellet was layered on 0.8 M/1.0 M/1.2 M sucrose after extensive re-suspension in 0.25 M sucrose. After ultracentrifugation at 70,000 × g, 1.0 M/1.2 M sucrose interface was collected and treated with 0.4% Triton X-100 for 30 min at 4 °C. Triton X-100-insoluble fraction was collected as PSD fraction. Protein concentration was measured by BCA method (Pierce). The same amount of the protein samples were separated by SDS/PAGE and transferred to polyvinylidene difluoride membrane. The membrane was cut into three pieces at 130 kDa and 60kDa molecular weight and reacted with the antibodies for GluR1 (4) and NR2B (4) subunits, and actin (Chemicon), respectively. For enhanced chemiluminescence detection, secondary antibody conjugated with horseradish peroxidase and Western Lightning chemiluminescence reagent (PerkinElmer) were used. For immunoblotting with NR2A, GluR2, and GluR3 subunits, membranes corresponding to each protein molecular weight were used. Purification of PSD fraction was further confirmed by immunoblotting for actin in each trial. The same immunoreactivity was obtained in left and right PSD fractions.

Tissue Preparation for SDS-FRL. Five days after the VHC transection, mice were anesthetized by pentobarbital (60 mg/kg i.p.) and

trans-cardially perfused with 25 mM PBS solution (pH 7.4), followed by a fixative containing 0.5% PFA, and 1.0% picric acid in 0.1 M PB (pH 7.4) for 12 min. To strictly control fixation conditions, 25 mM PBS solution was perfused again to remove remaining fixatives. After perfusion, the brains were immediately removed, and 150-μm-thick coronal slices were cut from the left and right dorsal hippocampi by a Microslicer (Dosaka). To compare the left and right side in the same condition, the same level of the dorsal hippocampal slice were used (approximately bregma, −1.94 mm). The slices were cryo-protected with 10% glycerol in 0.1 M PB, followed by 1 h 20% glycerol and overnight 30% glycerol in PB before high-pressure freezing.

The sections were then frozen by a high-pressure freezing machine (HPM 010; Bal-Tec) and fractured with double replica method in a freeze etching system (BAF 060; Bal-Tec). To compare the left and right side in the same condition, replicas from the left and right hippocampi were fractured at the same time. The fractured faces were replicated by carbon (5 nm) with an electron beam gun from overhead and shadowed by platinum/carbon (2 nm) positioned at a 45° angle unidirectionally, followed by carbon (20 nm) applied from overhead. The pieces of replica were transferred to 2.5% SDS containing 20% sucrose in 15 mM Tris buffer (pH 8.8). After the SDS treatment for 20 h at 80 °C with shaking, replicas were washed with three changes of washing buffer (0.01% BSA, 0.1% Tween 20 in 25 mM TBS solution, pH 7.4), and blocked with 5.0% BSA in the washing buffer. The replicas were then reacted with primary antibodies, in 1.0% BSA in the washing buffer. For GluR1 labeling, polyclonal rabbit antibody for GluR1 (extracellular epitope, 5.0 μg/ml) was used for 48 h at room temperature. For NR2B labeling, polyclonal rabbit (4) (extracellular epitope, 2.0 μg/ml) and guinea pig (intracellular epitope) antibodies (4) (2.0 μg/ml) were used respectively for 48 h at 4 °C, and for NR2A labeling polyclonal rabbit antibody (4) (0.5 μg/ml) were used for 12 h at 4 °C. The replicas were then washed three times with the washing buffer, blocked with 5% BSA in the washing buffer for 1 h, and incubated with secondary antibodies for 2 h at room temperature. A 1:30 dilution of goat anti-rabbit IgG coupled to 5-nm gold particles (British Biocell International) was used for GluR1, and NR2B (extracellular epitope) antibodies, and 1:30 dilution of goat anti-guinea pig IgG coupled to 10-nm gold particles (British Biocell International) was used for NR2B antibody (intracellular epitope). To mark synaptic sites, the replicas reacted with the GluR1 (extracellular epitope) antibody was sequentially labeled with mouse monoclonal NR1 antibody (extracellular epitope; Chemicon), then anti-mouse IgG coupled to 10-nm gold particles. After immuno-gold labeling, the replica was immediately rinsed three times with washing buffer, washed twice with distilled water, and picked up onto grids coated with pioloform (Agar Scientific). The central SR was observed by a Tecnai 12 electron microscope (FEI). Clusters of IMPs on E-face, typical for postsynaptic sites, that contain at least one NR1, NR2A, or NR2B labeling were analyzed as synaptic IMPs.

Rabbit antibody against extracellular epitope of GluR1 was raised against the amino acid residues 345–362 of the rat GluR1 (C-RFEGLTGNVQFNEKG), followed by affinity purification with the same peptide. Subsequently, the antibody was absorbed by GluR2 specific peptide (C-QVEGLSGNIKFDQNGKR) to avoid undesired contamination of GluR2 reacting antibodies. Specificity of the antibody was verified by immunoblotting (Fig. S8) and replica immunostaining of GluR1 KO animals (5).

Post-Embedding Immuno-Gold Labeling. For post-embedding labeling, small tissue blocks of the middle CA1 area (0.5 × 1.5 mm) were trimmed from the 500-μm-thick slices of the dorsal left and right hippocampus and cryoprotected in 10%, 20%, and 30% glycerol in 0.1 mM PB (pH 7.4) overnight. They were then frozen by plunging into liquid propane (−185 °C) in a cryo-fixation unit (EM CPC; Leica). Freeze substitution and low-temperature embedding in lowicryl HM20 were performed as described previously (3). The samples were immersed in 1% uranyl acetate dissolved in anhydrous methanol (−90 °C, 24 h) in a cryo-substitution unit (EM AFS; Leica). The temperature was then increased (4 °C/h) from −90 °C to −45 °C. The samples were washed three times with anhydrous methanol and infiltrated with lowicryl HM20 resin (Polysciences) at −45 °C with a progressive increase in the ratio of resin to methanol. Polymerization was performed with UV light (360 nm) at −45 °C for 24 h and 0 °C for 36 h. Lowicryl-embedded blocks were cut into 15 serial ultra-thin sections (70 nm thickness) and picked up onto single slot nickel grids coated with pioloform. Immunoreactions were carried out on a Leica EM IGL automated immuno-gold labeling instrument. First, the sections were incubated in blocking solution (2% human serum albumin in TBS solution with 0.1% Triton X-100) for 30 min. Then, for GluR1 labeling, 5 μg/ml anti-C terminus antibody (6) was added in the blocking solution. For NR2B labeling, 10 μg/ml anti-N terminus antibody (3, 4) and anti-C terminus antibody (3, 4) were mixed in the blocking solution. In both cases, the sections were reacted for 12 h at room temperature. After several washes with TBS solution for 30 min, the sections were incubated in goat anti-rabbit IgG coupled to 5-nm gold particles (British Biocell International) diluted 1:30 in a blocking solution containing polyethylene glycol (molecular weight, 7,500 kDa; 5 mg/ml) for 3 h. Then the sections were washed in ultra-pure water, contrasted with uranyl acetate, and observed by a Tecnai 10 electron microscope or EM208S electron microscope. Synaptic areas were calculated by total PSD length appeared in the serial images multiplied by 70 nm thickness.

Counting of Synaptic Numbers per Volume in Naïve and VHCT Mice. The number of synapses in a given area of CA1 SR was quantified by the "dissector method" as described previously (3). Briefly, in this method, two serial photo images were compared, and only synapses that were not found in the first image but appeared in the second were counted. First, naïve and VHCT mice were trans-cardially perfused with PBS solution followed by fixation with 4.0% paraformaldehyde supplemented with 0.1% glutaraldehyde. Brains were removed and 50-μm coronal sections were cut with a micro-slicer. After osmification and dehydration, and then flat embedding, 15 serial ultra-thin sections with 70-nm thickness were cut from the middle CA1 area of naïve and VHCT mice. EM pictures (with negatives) were taken from corresponding areas of each section with magnification ×6,300 (Fig. S6). The negatives were printed on A3-size paper, and newly appeared synapses in the second to 15th sections were counted. Three different areas from one animal were analyzed and averaged. Synaptic numbers per volume (number/μm^3) were calculated by dividing the number of synapses by measured area and by thickness of the sections (70 nm).

1. Fukata M, *et al.* (2001) Involvement of IQGAP1, an effector of Rac1 and Cdc42 GTPases, in cell-cell dissociation during cell scattering. *Mol Cell Biol* 21:2165–2183.
2. Kawakami R, *et al.* (2003) Asymmetrical allocation of NMDA receptor epsilon2 subunits in hippocampal circuitry. *Science* 300:990–994.
3. Wu Y, *et al.* (2005) Target-cell-specific left-right asymmetry of NMDA receptor content in schaffer collateral synapses in epsilon1/NR2A knock-out mice. *J Neurosci* 25:9213–9226.
4. Watanabe M, *et al.* (1998) Selective scarcity of NMDA receptor channel subunits in the stratum lucidum (mossy fibre-recipient layer) of the mouse hippocampal CA3 subfield. *Eur J Neurosci* 10:478–487.
5. Zamanillo D, *et al.* (1999) Importance of AMPA receptors for hippocampal synaptic plasticity but not for spatial learning. *Science* 284:1805–1811.
6. Inamura M, *et al.* (2006) Differential localization and regulation of stargazin-like protein, gamma-8 and stargazin in the plasma membrane of hippocampal and cortical neurons. *Neurosci Res* 55:45–53.

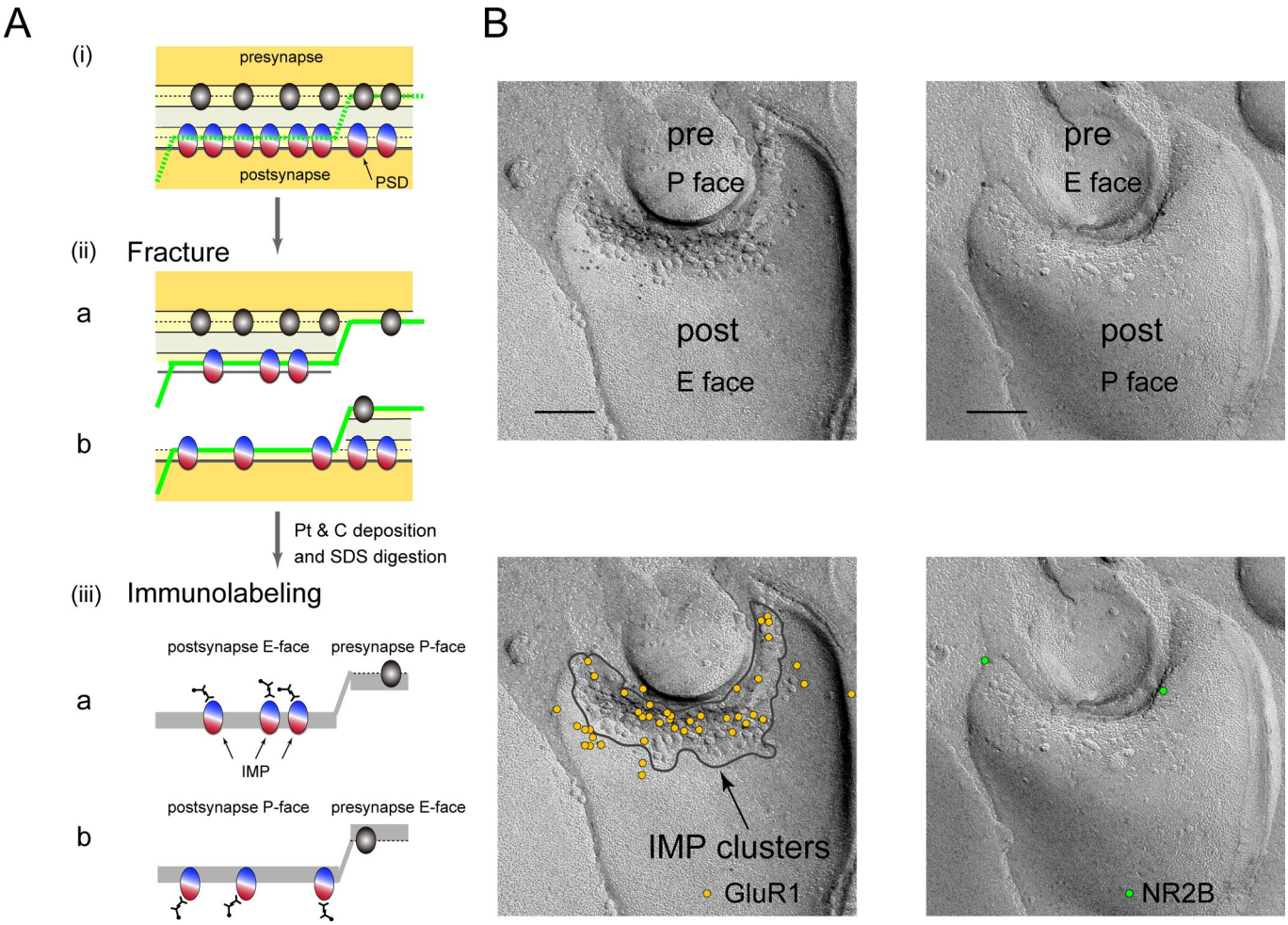

Fig. S1. EM examination of SDS-digested freeze-fracture replica samples for GluR1 and NR2B in CA1 SR. (*A*) Procedure of SDS-FRL immuno-labeling. Lipid bi-layers of presynaptic and postsynaptic membranes are closely apposed after fixation of the tissue (*i*). Fracturing process breaks the lipid bilayer into two faces (*ii*). The fractured faces were replicated by deposition of platinum and carbon, and then the opposite faces were digested by SDS. Treatment of SDS reveals membrane molecule on either the protoplasmic face (P-face) or exoplasmic face (E-face), resulting in sensitive detection by antibodies (*iii*). Postsynaptic E-face glutamatergic PSD areas deposited by platinum and carbon are recognized as intramembrane particles (IMPs). (*B*) An example of partial fracture of a synapse. Two faces of replica of the same synapse are displayed (*Upper*). Immuno-gold particles (5 nm) for GluR1 are observed within and around an IMP cluster (demarcated by gray line) on the E-face of spine head (post) next to P-face of presynaptic axon terminal (pre). On the corresponding P-face, immuno-gold particles (10 nm) for NR2B are observed. (Scale bars, 100 nm.) Immuno-gold particles for GluR1 (5 nm) on the E-face and those for NR2B (10 nm) on the corresponding P-face are shown in yellow and green dots, respectively (*Lower*).

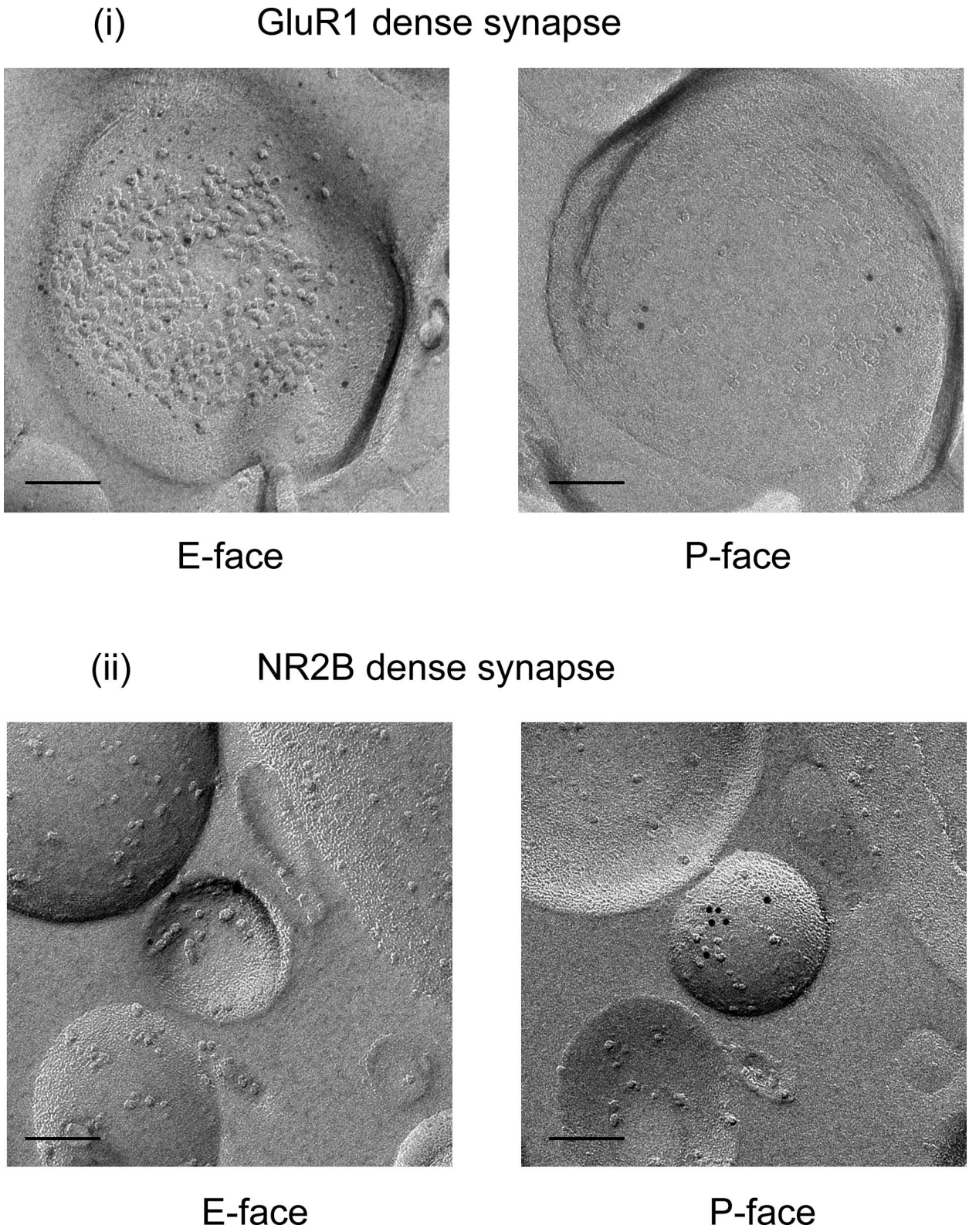

Fig. S2. Inverse correlation between NR2B and GluR1 densities in individual synapses (raw data of Fig. 3*A*). Examples of paired SDS-FRL from GluR1 dense (*i*) and NR2B dense (*ii*) synapses in VHCT mice (both 5 nm). Immuno-gold particles for NR1 (10 nm) are also observed on the E-face (Scale bars, 100 nm).

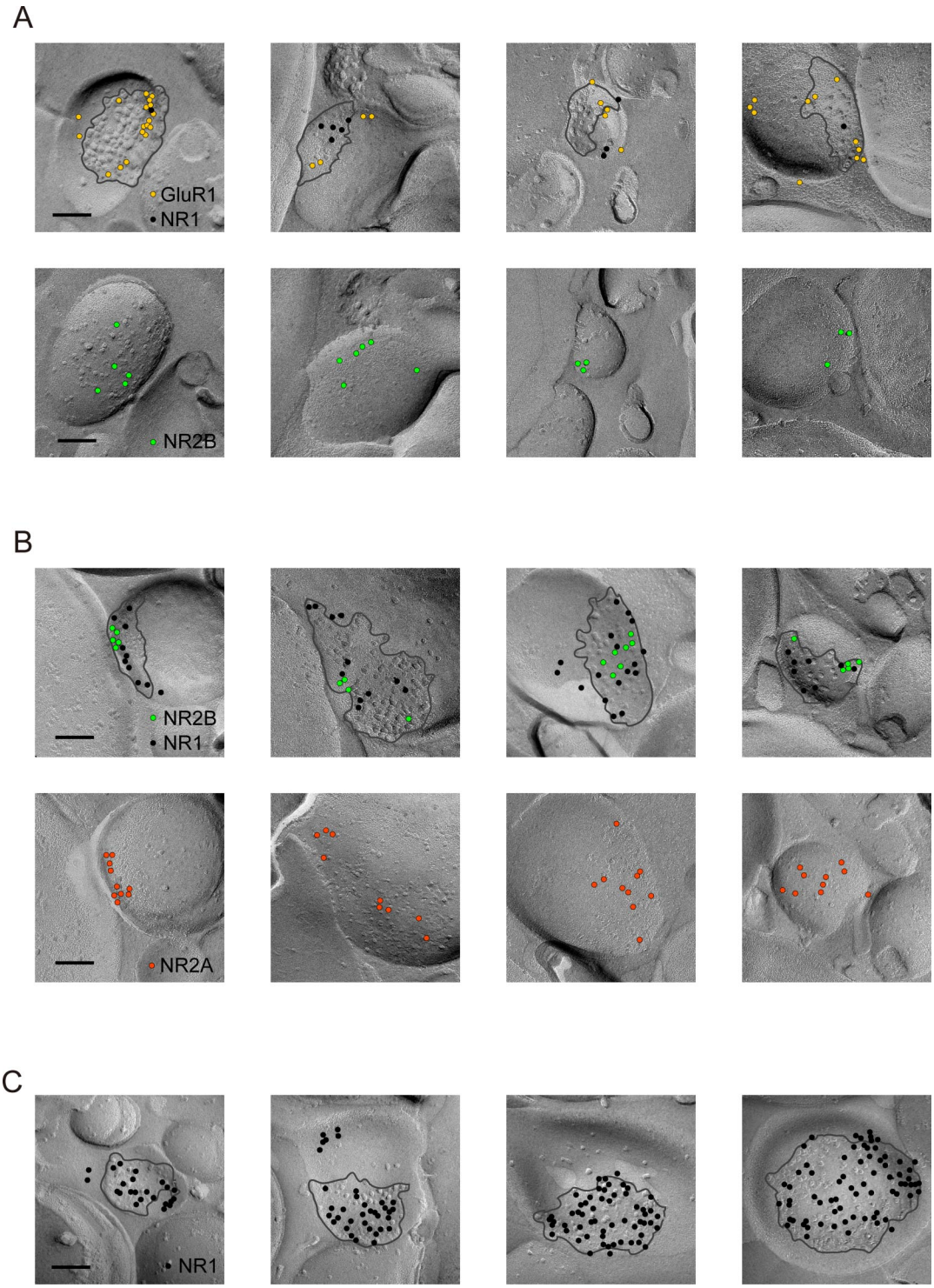

Fig. S3. Examples of SDS-FRL in CA1 SR of mice (*A*) Immuno-gold particles (5 nm) for GluR1 are observed within and around an IMP cluster (demarcated by gray line) on the E-face (*Upper*) of spine head. Immuno-gold particles (10 nm) for NR1 are also observed on the IMP cluster. On the corresponding P-face (*Lower*), immuno-gold particles (10 nm) for NR2B are observed showing a distribution pattern complementary to that of GluR1 (Scale bars, 100 nm). Color codes are as described. (*B*) Immuno-gold particles (5 nm) for NR2B are observed within and around an IMP cluster (demarcated by gray line) on the E-face (*Upper*) of spine head. Immuno-gold particles (10 nm) for NR1 are also observed on the IMP cluster. On the corresponding P-face (*Lower*), immuno-gold particles (5 nm) for NR2A (red) are observed. Note that NR2A subunits (shown in red) showed more scattered distribution than NR2B subunits (Scale bars, 100 nm). (*C*) Immuno-gold particles (5 nm) for NR1 are observed within and around an IMP cluster (demarcated by gray line) on the E-face (*Upper*) of spine head. Single labeling for NR1 gives much more intense immuno-gold signals than sequential labeling for NR1 that followed to GluR1 (*A*) or NR2B (*B*) labeling. In most cases, NR1 subunits are uniformly distributed within IMP clusters.

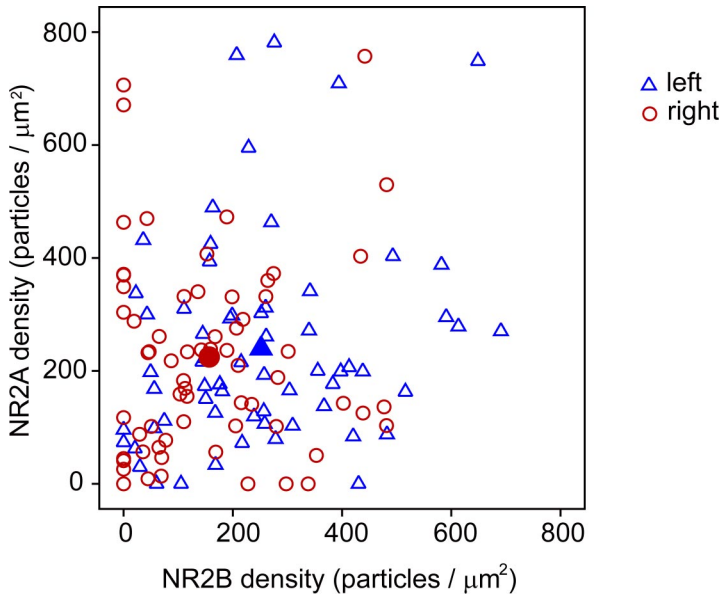

Fig. S4. No correlation is seen between labeling densities for NR2A and NR2B subunits in VHCT mice. Data from two VHCT mice were pooled as no significant difference in distribution was detected between corresponding groups. Note that labeling density for NR2B is higher on the left (blue) than on the right (red). We did not detect a significant correlation between the labeling densities for NR2A and NR2B subunits in VHCT mice ($n = 63$ for left, $n = 64$ for right). Moreover, no significant left-right difference in NR2A labeling was detected. Significant left-right difference in NR2B density was detected in the same pair of replicas ($P < 0.005$, Mann-Whitney test). Filled blue triangle and red circles represent the average densities of left and right synapses, respectively.

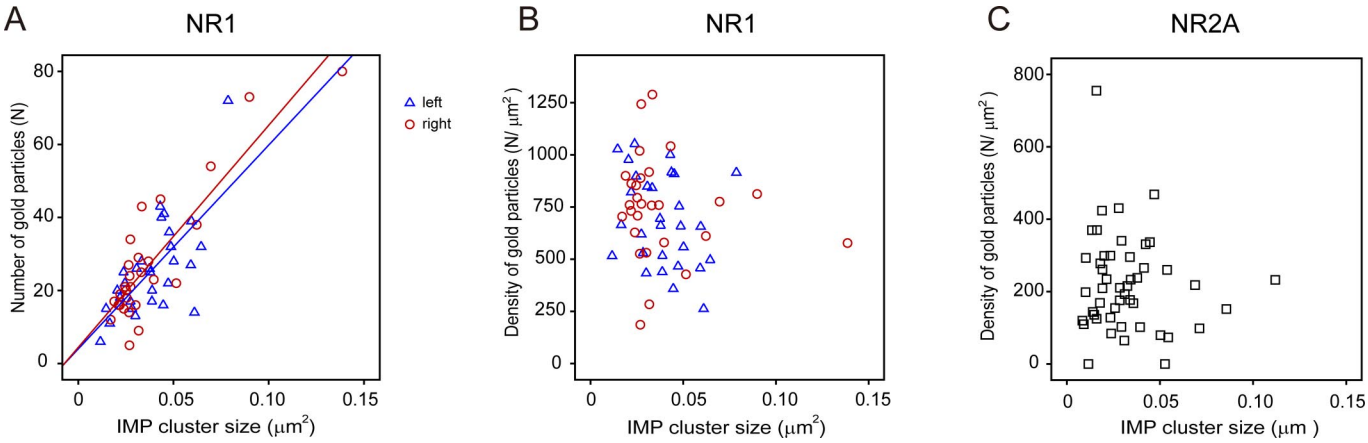

Fig. S5. Relationship of NR1 subunit number (*A*), NR1 density (*B*), and NR2A density (*C*) to IMP cluster size measured from SDS-FRL samples of VHCT mouse. For NR1 labeling, in both left and right sides, number of immunolabeling showed strong correlation to IMP cluster size (*Left*, $R_p = 0.693$, $n = 29$, $P < 0.01$; *Right*, $R_p = 0.879$, $n = 28$, $P < 0.01$). However, labeling densities did not show significant correlation to IMP cluster size. Moreover, there were no significant differences between left and right NR1 labeling densities (Mann-Whitney test). No correlation was found in the NR2A density/IMP cluster size relationship ($n = 49$).

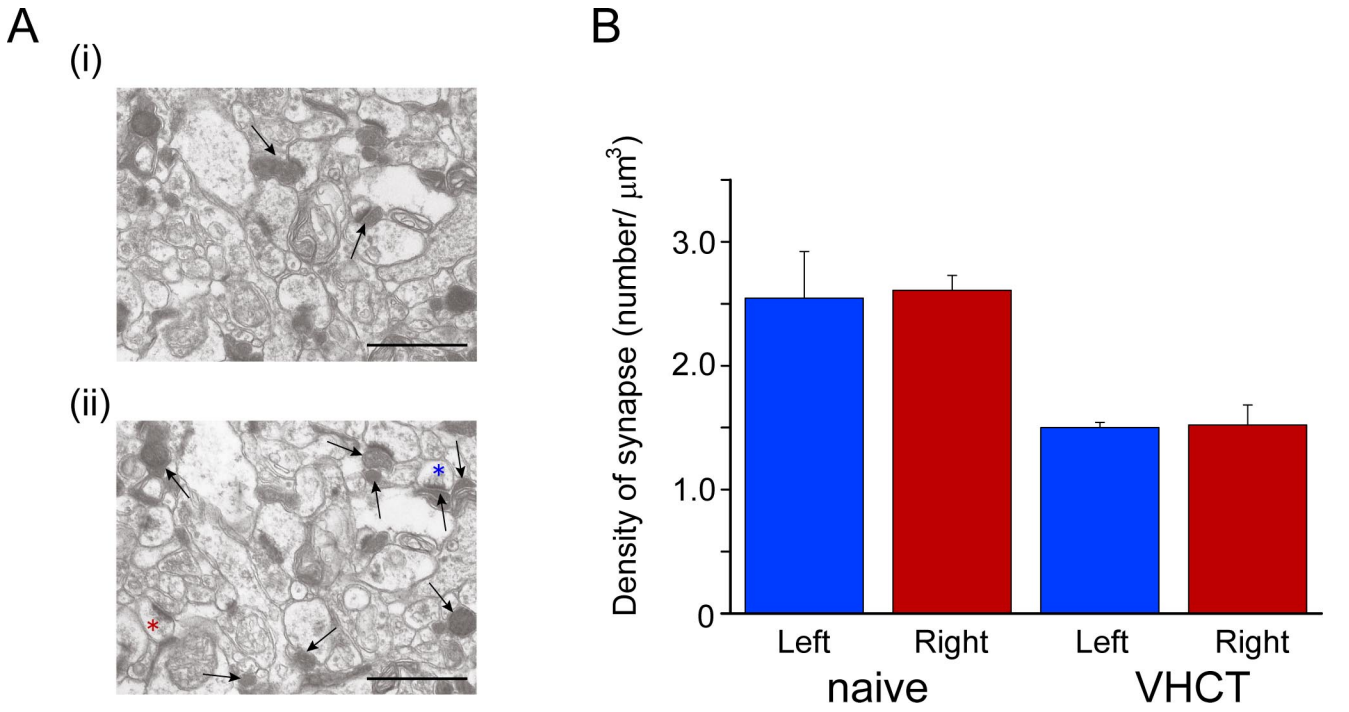

Fig. S6. Synaptic numbers of area CA1 of naïve and VHCT mice. (*A*) Synaptic numbers were calculated by the dissector method (3). Briefly, in this method, two serial photo images were compared, and only synapses not found in the first image (*i*), but that appeared in the second (*ii*), were counted (shown with asterisks). Degenerating synapses and axon terminals of contralateral inputs are pointed by arrowheads. Synapses receiving ipsilateral and contralateral axons marked with red and blue asterisks, respectively. (*B*) Three different areas from one animal were analyzed and averaged. In both left and right sides, VHCT mouse shows approximately 40% decrease of intact synapses. This indicates that approximately 60% and 40% of dorsal CA1 synapses are innervated by ipsilateral and contralateral sides of CA3 neurons, respectively. Error bars indicate SD.

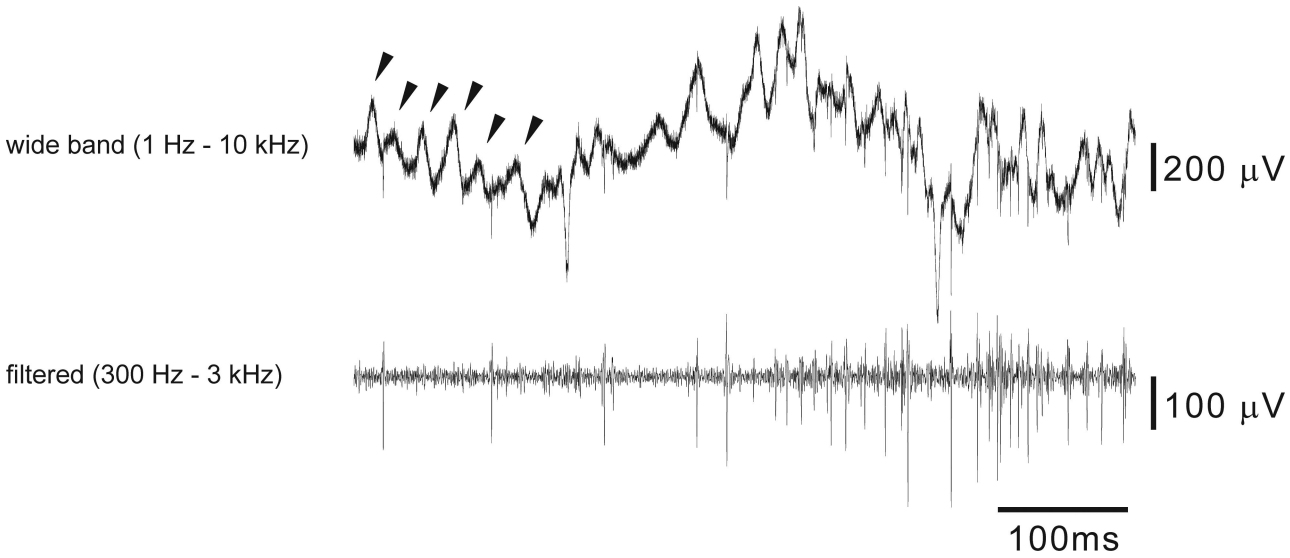

Fig. S7. Extracellular electrophysiological signature of CA3 neural activity. In addition to the stereotaxic coordinate, electrophysiological signal was monitored through the virus-containing fine glass pipette. Electrode positioning at the CA3 pyramidal cell layer is recognized by the emergence of the characteristic gamma band oscillations (arrowheads, *Upper*), as well as by the presence of multiunit activity (*Lower*).

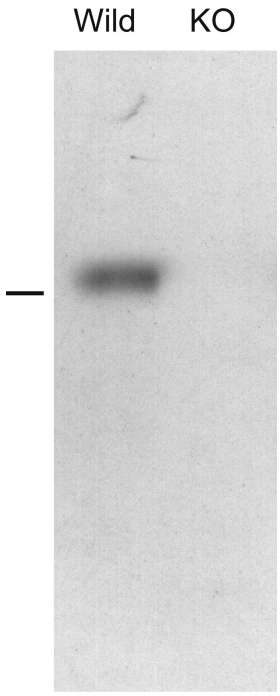

Fig. S8. Specificity of the GluR1 antibody used for replica labeling. The same amount of protein of frontal cortex from WT (Wild) and GluR1-KO mouse (KO) was immuno-blotted with the GluR1 antibody. Line (*Left*) represents the location of protein marker (105 kDa). Note that immunoreactive band corresponding to GluR1 molecular weight in WT completely disappears in KO.